TISSUE ENGINEERING: Part A
Volume 19, Numbers 1 and 2, 2013

DOI: 10.1089/ten.tea.2011.0728

Effects of B-Cell Lymphoma 2 Gene Transfer to Myoblast Cells on Skeletal Muscle Tissue Formation Using Magnetic Force-Based Tissue Engineering

Masanori Sato, M.Eng., Akira Ito, Ph.D., Hirokazu Akiyama, Ph.D., Yoshinori Kawabe, Ph.D., and Masamichi Kamihira, Ph.D.

Tissue-engineered skeletal muscle should possess a high cell-dense structure with unidirectional cell alignment. However, limited nutrient and/or oxygen supply within the artificial tissue constructs might restrict cell viability and muscular functions. In this study, we genetically modified myoblast cells with the anti-apoptotic B-cell lymphoma 2 (*Bcl-2*) gene and evaluated their function in artificial skeletal muscle tissue constructs. Magnetite cationic liposomes were used to magnetically label C2C12 myoblast cells for the construction of skeletal muscle bundles by applying a magnetic force. Bcl-2-overexpressing muscle bundles formed highly cell-dense and viable tissue constructs, while muscle bundles without Bcl-2 overexpression exhibited substantial necrosis/apoptosis at the central region of the bundle. Bcl-2-overexpressing muscle bundles contracted in response to electrical pulses and generated a significantly higher physical force. These findings indicate that the incorporation of anti-apoptotic gene-transduced myoblast cells into tissue constructs significantly enhances skeletal muscle formation and function.

Introduction

Regeneration of adult skeletal muscle is mainly attributable to myoblast cells. In response to growth or tissue regeneration stimuli, myoblast cells proliferate and fuse to form multinucleated myotubes. Thus, skeletal muscle is composed of fused and differentiated myoblasts with a high cell density. To construct functional artificial skeletal muscles, tissue-engineered skeletal muscles should reproduce the structural features of the native muscle, that is, densely packed, uniformly aligned muscle fibers, surrounded by an extracellular matrix (ECM). The most common approach is a tissue formation procedure that is mediated by naturally derived hydrogels, such as collagen type I and Matrigel, where three-dimensional (3D) tissue formation can be induced from a mixture of myoblast cells and ECM precursors. Although hydrogel-based muscle tissue constructs have been successfully engineered to contain aligned myotubes,[1–4] cells mainly distribute at the tissue periphery and are much less compact than native skeletal tissues, which can limit further development of functional skeletal muscle tissue.

To date, several new strategies for the fabrication of skeletal muscle tissues have been developed.[5–10] Dennis *et al.*[5] reported a scaffold-free approach for 3D tissue fabrication, which involves the self-assembly of myoblast cells on a silicone surface. Saxena *et al.*[7] showed vascularized skeletal muscle constructs using isolated myoblasts immobilized on synthetic biodegradable polymers. Gawlitta *et al.*[8] presented hydrogel-based skeletal muscle tissue-engineered constructs using collagen type I gel and Matrigel anchored by Velcro. Moon du *et al.*[9] demonstrated improved contractile force generation of engineered skeletal muscle tissue constructs using collagen-based acellular tissue scaffolds. Singh *et al.*[10] proposed 3D supermacroporous cryogel as a scaffold for skeletal muscle tissue fabrication. All these fabrication techniques for skeletal muscle tissue constructs were material-based techniques, and less volume of cells was occupied in the tissue constructs. Alternatively, we previously developed a tissue engineering technique, called magnetic force-based tissue engineering (Mag-TE), where cells labeled with magnetic nanoparticles are used to fabricate tissue constructs by applying magnetic force.[11–13] In Mag-TE, magnetically labeled target cells are accumulated using a magnet, and subsequent stratification of cells is promoted by magnetic force, leading to the formation of 3D tissue-like constructs. Since this technique enables the considerably cell-dense structures with cells attached to each other, we applied this technique to fabricate artificial skeletal muscle tissue constructs, including skeletal muscle bundles.[14,15]

Under a highly packed cell-dense environment, cells may encounter a deficiency in oxygen availability, resulting in hypoxia. This may result in decreased cell viability and, thus, hinder the fabrication of functional skeletal muscle tissues

Department of Chemical Engineering, Faculty of Engineering, Kyushu University, Fukuoka, Japan.

with substantial mass and thickness. To avoid hypoxic conditions, numerous attempts have been made to promote tissue vascularization after transplantation *in vivo*.[13,16–18] In general, although it takes at least several days for the induction and formation of blood vessels, cells can only survive under hypoxic conditions for a short period.[19] Thus, *in vitro* fabrication and long-term culture of large tissue constructs remain challenging.

B-cell lymphoma 2 (Bcl-2) protein is known as a critical regulator of apoptosis.[20] A previous study demonstrated that Bcl-2 inhibits intrinsic mitochondrial-dependent cell death by conserving the integrity of the outer mitochondrial membrane.[21] Bcl-2 overexpression has been shown to promote cell survival and inhibit cell death induced by apoptotic conditions, such as nutrient depletion[22] and hypoxia.[23] From these reports, we hypothesized that the stress-resistant effects of Bcl-2 may improve the formation of artificial skeletal muscle tissue constructs with a high cell density, thereby enabling them to be more functional under stressful conditions. In this study, an inducible expression *Bcl-2* gene cassette was introduced into mouse myoblast C2C12 cells by retroviral transduction, and the effects of *Bcl-2* gene transfer on skeletal muscle tissue formation and muscular functions of Mag-TE tissue constructs were examined.

Materials and Methods

Cell culture

Mouse myoblast C2C12 cells were grown in Dulbecco's modified Eagle's medium (DMEM) supplemented with 10% fetal bovine serum (FBS), 100 U/mL penicillin G potassium, and 0.1 mg/mL streptomycin sulfate. To induce myogenic differentiation, the medium was changed to DMEM supplemented with 2% calf serum (CS) for a two-dimensional (2D) cell culture or 0.4% Ultroser G (Pall, East Hills, NY) for a 3D tissue culture, and the antibiotics. Cells were cultured at 37°C in a 5% CO_2 incubator. 293FT cells were used as a producer for retroviral vectors based on Moloney murine leukemia virus (MoMLV) and were cultured as previously described.[4]

Cloning of mouse Bcl-2 gene and plasmid construction

Total RNA was extracted from mouse blood cells using a QuickPrep Total RNA Extraction Kit (GE Healthcare, Buckinghamshire, United Kingdom). Isolated RNA was reverse transcribed with ReverTra Ace reverse transcriptase (Toyobo, Osaka, Japan). A DNA fragment of mouse *Bcl-2* gene was amplified by polymerase chain reaction (PCR) using the following primers: 5′-CGGAATTCTTTTCGGGGAAGGATG GC-3′ (forward) and 5′-AACTGCAGTGGGGCAGGTTTGTC GACC-3′ (reverse), which append *Eco*RI and *Pst*I sites (underline). PCR was initiated using KOD-plus DNA polymerase (Toyobo) at 94°C for 2 min, followed by 35 amplification cycles at 94°C for 15 s, 55°C for 30 s, and 68°C for 45 s. Then, the PCR product was digested with *Eco*RI and *Pst*I and ligated into *Eco*RI- and *Pst*I-digested pcDNA4/E-cad-IRES-EGFP[24] to generate pcDNA4/Bcl-2-IRES-EGFP. The DNA sequence of *Bcl-2* was confirmed using a DNA sequencer (Prism 3130 Genetic Analyzer; Applied Biosystems, Foster City, CA).

MoMLV-derived mouse stem cell virus (MSCV)-based retroviral vectors were used for gene transfer into C2C12 cells. The Tet-On system (Clontech, Mountain View, CA) was incorporated into the retroviral vectors for inducible expression of the *Bcl-2* gene. For retroviral vector production, two plasmids, pQMSCV/EGFP-CMV-rtTA-WPRE and pQMSCV/EGFP-TRE-Bcl2-WPRE, were constructed. pQMSCV/EGFP-CMV-rtTA-WPRE encodes a constitutive expression cassette for a transactivator (*rtTA*) that is activated by the addition of doxycycline (Dox). pQMSCV/EGFP-TRE-Bcl2-WPRE encodes an expression cassette for *Bcl-2* gene, including a tet-responsive element, such that *Bcl-2* expression is promoted by the activation of rtTA. These plasmids included an enhanced green fluorescent protein (*EGFP*) gene under the control of viral long terminal repeat (LTR) promoters to evaluate the viral titer. To construct pQMSCV/EGFP-CMV-rtTA-WPRE, a DNA fragment encoding the *EGFP* gene was amplified from pIRES-EGFP (Clontech) by PCR, and the resulting fragment was ligated into *Eco*RI- and *Xho*I-digested pQMSCV/CMV-VEGF-IRES-EGFP[13] to generate pQMSCV/EGFP. Next, the woodchuck hepatitis virus post-transcriptional regulatory element (WPRE) sequence from pMSCV/GΔAhEpoW[25] was ligated into *Cla*I-digested pQMSCV/EGFP, resulting in pQMSCV/EGFP-WPRE. Thereafter, the cytomegalovirus (CMV) promoter and the *rtTA* sequences from pTet-On Advanced (Clontech) were ligated into *Xho*I- and *Cla*I-digested pQMSCV/EGFP-WPRE to generate pQMSCV/EGFP-CMV-rtTA-WPRE. For the construction of pQMSCV/EGFP-TRE-Bcl2-WPRE, a tet-responsive promoter from pTRE-Tight (Clontech) was ligated into *Xho*I- and *Cla*I-digested pQMSCV/EGFP-WPRE to generate pQMSCV/EGFP-TRE-WPRE. Subsequently, a *Bcl-2* gene fragment from pcDNA4/Bcl-2-IRES-EGFP was ligated into *Bam*HI- and *Not*I-digested pQMSCV/EGFP-TRE-WPRE, resulting in pQMSCV/EGFP-TRE-Bcl2-WPRE.

Retroviral vector production and infection

Retroviral vectors pseudotyped with vesicular stomatitis virus G protein (VSV-G) were produced by transient transfection of 293FT cells with three plasmid DNAs, comprising a retroviral vector plasmid (pQMSCV/EGFP-CMV-rtTA-WPRE or pQMSCV/EGFP-TRE-Bcl2-WPRE), pcDNA4-gag/pol, and pLP/VSV-G,[26] using the lipofection reagent Lipofectamine 2000 (Invitrogen). The culture medium containing viral vector particles was filtered through a 0.45-μm cellulose acetate filter (Advantec, Tokyo, Japan) and used for retroviral infection.

For retroviral infection, C2C12 cells (2.5×10^5 cells) were seeded into a 100-mm tissue culture dish (Greiner Bio-one, Frickenhausen, Germany) and cultured for 24 h. Subsequently, the medium was replaced with 10 mL of retroviral solution, comprising a 1:1 mixture of two media containing the retroviral vectors encoding the *rtTA* and inducible *Bcl-2* gene expression cassettes. The cells were then cultured in the presence of polybrene (8 μg/mL) for 6 h, resulting in the generation of C2C12 cells that were capable of Dox-inducible *Bcl-2* gene expression (designated as C2C12/Bcl-2 cells). All viral titers against C2C12 cells were in the range of 2.5–5.0×10^6 IU/mL at infection (multiplicity of infection = 5–10 for each vector).

Observation of myotubes contracted under electrical stimulation

Normal C2C12 (WT) and C2C12/Bcl-2 cells (1×10^5 cells/well) were cultured on four-well plates (Nalgen Nunc International, Rochester, NY) in 5 mL of growth medium (DMEM containing 10% FBS) for 2 days and were differentiated into myotubes in 5 mL of differentiation medium (DMEM containing 2% CS) for 7 days. These media with or without Dox were changed daily. On day 7, the differentiated myotubes in four-well plates were placed in a chamber for electrical stimulation (C-Dish; IonOptix, Milton, MA) and observed under an IX71 microscope (Olympus, Tokyo, Japan) applying electric pulses (voltage, 0.3 V/mm; width, 10 ms; frequency, 1 Hz). To estimate the percentages of myotubes contracted under electrical stimulation, 10 microscope fields in a well were randomly selected, and the numbers of myotubes that contracted and noncontracted with electrical stimulation were counted. Three wells under each condition were measured ($n=3$).

Hypoxic and serum-depletion cultures

C2C12/Bcl-2 cells (6×10^4 cells) were seeded into 35-mm cell culture dishes (Greiner Bio-one). After 3 h of incubation, the cells were washed with serum-free medium, replaced with 5 mL growth media with or without FBS, and incubated under normoxic (5% CO_2, 95% air) or hypoxic (1% O_2, 5% CO_2, 94% N_2) conditions. To investigate the effect of Bcl-2 overexpression on cell viability under these culture conditions, cells were cultured in the presence or absence of Dox (1 μg/mL) 1 day before cell seeding. The numbers of viable and dead cells were measured at 24 and 48 h using the trypan blue dye-exclusion method. To calculate growth ratio, viable cell numbers in each culture period were divided by the initial cell number.

Fabrication of skeletal muscle tissue constructs by Mag-TE

Magnetite cationic liposomes (MCLs) were prepared from colloidal magnetite (Fe_3O_4; average particle size, 10 nm) and a lipid mixture consisting of *N*-(α-trimethylammonioacetyl)-didodecyl-D-glutamate chloride, dilauroylphosphatidylcholine, and dioleoylphosphatidyl-ethanolamine, in a molar ratio of 1:2:2.[27] To prepare MCL-labeled C2C12 cells, 7×10^5 cells were seeded in 100-mm tissue culture dishes (Greiner Bio-one) containing 10 mL growth medium, in the presence of MCLs (magnetite concentration, 100 pg/cell), and incubated for 8 h to allow MCL uptake.

Artificial skeletal muscle tissue constructs were prepared as previously described.[14] Briefly, a polycarbonate cylinder was fixed at the center of the well of a 24-well ultralow-attachment culture plate (Corning, New York, NY). MCL-labeled C2C12 cells (1×10^6 cells) were seeded into the gap between the well wall and the cylinder, and a neodymium magnet (diameter, 30 mm; magnetic induction, 0.4 T) was placed under the well. Subsequently, the cells were cultured for 2 days to allow for the formation of a ring-shaped cellular construct. After 2 days of culture in growth medium, an ECM solution, consisting of 0.04 mL of type I collagen (1.1 mg/mL; Nitta Gelatin, Osaka, Japan), 0.05 mL of Matrigel (4.4 mg/mL; BD Biosciences, Franklin Lakes, NJ), and 0.01 mL of growth medium, was added to the well and the solution was subsequently replaced with culture medium. After 4 h of incubation, the cellular ring was removed from the polycarbonate cylinder and hooked around two stainless-steel minuten pins (Shiga, Tokyo, Japan), fixed 6 mm apart on a silicone rubber sheet in a 35-mm culture dish (day 0). To induce myogenic differentiation, the cellular rings were cultured in differentiation medium. The skeletal muscle tissue constructs, designated as muscle bundles, were cultured for 7 days. During the culture period, the number of ruptured bundles was counted daily. Concurrently, one to three intact muscle bundle samples were collected for biochemical analyses. Percentages of form retention for muscle bundles were estimated according to the Kaplan–Meier method,[28] as a considerable number of muscle bundle samples were collected during the culture period and used for biochemical analyses.

Measurement of total cell nuclei of muscle bundles

Muscle bundles were washed with phosphate-buffered saline (PBS), and the total number of nuclei was counted using NucleoCassette™ (Chemometec, Allerød, Denmark) and NucleoCounter™ (Chemometec). The percentage of remaining nuclei in the muscle bundles was calculated as follows: Percentage of remaining nuclei (%) = [(number of nuclei in muscle bundles on the indicated day)/(number of nuclei in muscle bundles on day 0)] × 100.

Histological study

The muscle bundles were washed thrice with PBS, fixed in 4% paraformaldehyde in PBS, and embedded in paraffin. Thin sections were prepared and stained with hematoxylin and eosin (H&E). Apoptosis in the muscle bundles was assessed using terminal deoxynucleotidyl transferase dUTP nick end labeling (TUNEL) assay kit (Roche, Mannheim, Germany). Slides were also double stained with Berlin blue[29] and counterstained with hematoxylin. The stained sections were observed under an IX71 microscope.

For fluorescence observation of the muscle bundles, the tissue constructs were fixed in 4% paraformaldehyde for 15 min, washed in PBS containing 0.2% Triton-X 100 for 15 min, and immersed in PBS containing 4′,6-diamidino-2-phenylindole (DAPI; Invitrogen) for 45 min. The specimens were observed under a BZ-9000 fluorescence microscope (Keyence, Tokyo, Japan).

Western blot analysis

Western blot analysis for Bcl-2, myosin heavy chain (MHC), myogenin, tropomyosin, and GAPDH were performed as previously described.[4,15] Briefly, cellular proteins were extracted by homogenization and freeze thawing. Protein samples (30 μg) were mixed with sodium dodecyl sulfate-polyacrylamide gel electrophoresis sample buffer containing 2-mercaptoethanol and boiled at 100°C for 5 min. Subsequently, the samples were electrophoresed in 7.5% (for MHC) or 12% acrylamide gel, and the separated proteins were transferred to a polyvinylidene fluoride membrane (GE Healthcare). After blocking with 5% skimmed milk in Tris-buffered saline containing 0.05% Tween 20 (TBS-T) at 4°C overnight, the membrane was incubated with a primary

antibody (sc-492 for Bcl-2; Santa Cruz Biotechnology, Santa Cruz, CA) for 1 h. The bound antibodies were detected using horseradish peroxidase-conjugated secondary antibodies (Santa Cruz Biotechnology) and a chemiluminescence detection kit (ECL detection system; GE Healthcare).

Creatine kinase activity

Creatine kinase activity was determined using a commercially available assay kit (CPK-II Test Wako; Wako Pure Chemical Industries, Tokyo, Japan) as previously described.[4,15]

Tension measurement

Carbon electrodes were placed 10 mm apart at the opposite sides of a tissue culture plate. A muscle bundle was hooked around two stainless-steel minuten pins (Shiga). One pin was attached to a force transducer (AE-801; SonorOne, Sausalito, CA), and the other was fixed to a silicon rubber sheet placed at the bottom of the culture plate. Electrical pulses were computer controlled with specially designed LabView software (National Instruments, Austin, TX). For measuring twitch contractions, the tissue sample was stimulated with an electrical pulse of 20 V with a width of 10 ms. For measuring tetanic contractions, the tissue sample was stimulated with electrical pulses with the following properties: voltage, 20 V; width, 10 ms; frequency, 50 Hz; and duration, 2 s.

Statistical analysis

Statistical comparisons were evaluated using the Mann–Whitney rank sum test. The one-way analysis of variance was used for the evaluation of hypoxic and serum-depletion cultures. For percentages of form retention estimated by the Kaplan–Meier method, statistical comparisons were performed using the log-rank test. Differences in all statistical comparisons were considered significant at levels of p values < 0.05.

Results

Inducible expression of Bcl-2 gene in C2C12 cells

In this study, we used a retroviral vector system that enabled inducible expression of the *Bcl-2* gene. Since the vectors encode an *EGFP* gene controlled by the viral LTR promoter, EGFP expression from the vector-transduced C2C12 cells could be observed by fluorescence microscopy (Fig. 1D). To investigate inducible *Bcl-2* gene expression, the cells were cultured in the presence or absence of Dox, and Bcl-2 expression was detected by western blotting (Fig. 1E). Bcl-2 protein bands, with a molecular weight of ~26 kDa, were detected in cells cultured with Dox addition [C2C12/Bcl-2 (Dox+)], but no bands were seen in the cells without Dox addition [C2C12/Bcl-2 (Dox−)], indicating the successful generation of C2C12 cells with Dox-inducible Bcl-2 expression.

To investigate whether the genetically modified cells retain their differentiation ability, multinucleated myotube formation was induced in C2C12/Bcl-2 cells by the addition of differentiation medium with or without Dox addition. As shown in Figure 1G and I, no morphological differences were seen in myotubes from C2C12/Bcl-2 (Dox+) and C2C12/Bcl-2 (Dox−) cells. Furthermore, to examine the contractility of myotubes induced from C2C12/Bcl-2 cells, myotubes were stimulated with electrical pulses. As shown in Figure 1J, cell contractility did not change between the cells before and after the gene transfer. These results indicate that Bcl-2 overexpression did not affect the differentiation of C2C12 cells.

Effects of Bcl-2 overexpression on cell growth and death under hypoxic and serum-depletion conditions

To investigate whether Bcl-2 overexpression facilitates the promotion of cell survival and protection against cell death under hypoxic and nutrient depletion conditions, C2C12/Bcl-2 cells were cultured in hypoxic (1% O_2) or nutrient-deprived (without FBS supplementation) conditions in the presence or absence of Dox. Under normal culture conditions, Bcl-2 overexpression did not affect cell growth or cell death (data not shown). Under hypoxic conditions, Bcl-2 overexpression slightly increased cell growth, and there was a 63% reduction of cell death ($p < 0.05$) compared with C2C12/Bcl-2 (Dox−) cells (Fig. 2A). Under serum-depleted conditions, C2C12/Bcl-2 (Dox+) cells did not proliferate, but maintained ~85% of the initial cell number after 48 h culture periods; while the number of C2C12/Bcl-2 (Dox−) cells was reduced to below 70% (Fig. 2B). In addition, the percentage of cell death decreased, and cell viability was improved in C2C12/Bcl-2 (Dox+) cells (Fig. 2B). These results indicate that the Bcl-2-overexpressing C2C12 cells acquired a stress-resistant ability, which may facilitate cell survival in cell-dense environments of reconstructed 3D tissue constructs.

Fabrication of artificial skeletal muscle tissue constructs

To investigate the effect of *Bcl-2* gene transfer on engineered skeletal muscle tissue constructs, C2C12/Bcl-2 muscle bundles were fabricated using Mag-TE.[14,15] During differentiation culture, some skeletal muscle bundles ruptured because of the high degree of contraction. As shown in Figure 3A, C2C12/Bcl-2 (Dox−) muscle bundles exhibited a significantly higher percentage of rupture (39%) after 7 days of culture, whereas 84% of C2C12/Bcl-2 (Dox+) muscle bundles remained intact on day 7. To explore why there was a higher yield of C2C12/Bcl-2 (Dox+) muscle bundles, we compared the number of nuclei within C2C12/Bcl-2 (Dox+) and C2C12/Bcl-2 (Dox−) muscle bundles during differentiation culture. Significant differences were observed in the remaining nuclei between C2C12/Bcl-2 (Dox−) and C2C12/Bcl-2 (Dox+) muscle bundles from day 4, indicating that Bcl-2 overexpression reduced cell death within the tissue constructs, which helps prevent rupturing.

Structure of artificial skeletal muscle tissue constructs

We further examined the impact of *Bcl-2* gene transfer on the engineered skeletal muscle structure. Figure 4A shows a representative C2C12/Bcl-2 (Dox+) muscle bundle. The thickness of the C2C12/Bcl-2 (Dox+) muscle bundle on day 7 was ~300–400 μm, which was similar to the C2C12/Bcl-2 (Dox−) muscle bundles. Fluorescence microscopy of the skeletal muscle bundles stained with DAPI revealed that the

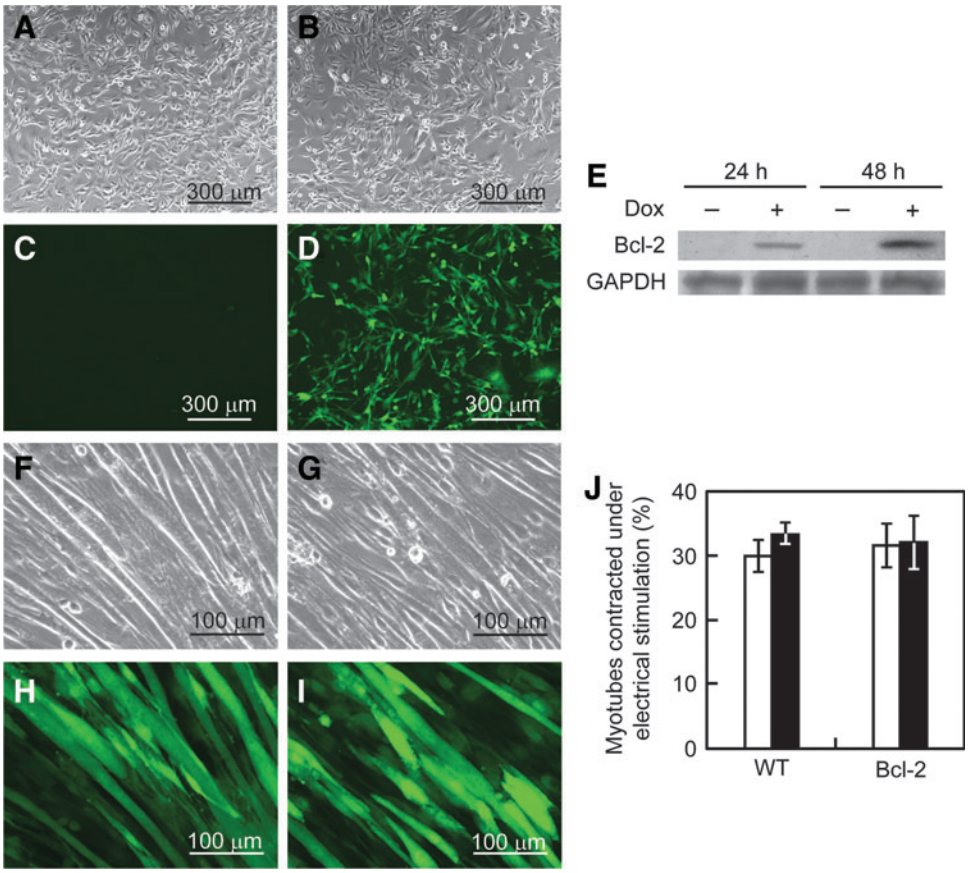

FIG. 1. Generation of C2C12/B-cell lymphoma 2 (Bcl-2) cells. **(A–D)** C2C12 cells were transduced with retroviral vectors incorporating the doxycycline (Dox)-inducible Bcl-2 expression system. Cells were observed by phase contrast **(A, B)** and fluorescence **(C, D)** microscopy before **(A, C)** and after **(B, D)** retroviral infection. **(E)** Bcl-2 expression analysis in C2C12/Bcl-2 cells by western blotting. Bcl-2 proteins were detected from the cells cultured in the presence or absence of Dox for 24 or 48 h. **(F–I)** The effect of Bcl-2 overexpression on skeletal muscle differentiation. After C2C12/Bcl-2 cells had reached a subconfluent state in growth medium, the medium was changed to differentiation medium and cultured for further 10 days. Cells cultured in the absence **(F, H)** or presence **(G, I)** of Dox were observed by phase contrast **(F, G)** and fluorescence **(H, I)** microscopy. **(J)** The effect of Bcl-2 overexpression on cell contractility. The percentages of myotubes contracted under electrical stimulation for normal C2C12 (WT) and C2C12/Bcl-2 (Bcl-2) cells were measured. Open columns, without Dox addition; closed columns, with Dox addition. The data are expressed as mean ± standard deviation (SD) ($n = 3$). Color images available online at www.liebertpub.com/tea

outermost cell layer consisted of longitudinally oriented and multinucleated myotubes (Fig. 4B, C). Moreover, the morphology and number of myotubes were similar for both C2C12/Bcl-2 (Dox−) and C2C12/Bcl-2 (Dox+) muscle bundles. In contrast, H&E staining of cross-sections of the bundles showed that C2C12/Bcl-2 (Dox−) muscle bundles consisted of an outer region with densely packed cells and a necrotic central region (Fig. 4D); while no substantial necrotic region was observed in C2C12/Bcl-2 (Dox+) muscle bundles (Fig. 4E). Furthermore, a significant number of TUNEL-positive cells were observed in C2C12/Bcl-2 (Dox−) muscle bundles (10.7% ± 1.5%) around the necrotic area at the central region (Fig. 4F), while C2C12/Bcl-2 (Dox+) muscle bundles exhibited a less number of TUNEL-positive cells (5.3% ± 1.1%) (Fig. 4G). These results indicate that Bcl-2 overexpression prevents cell death within the C2C12/Bcl-2 (Dox+) muscle bundles, especially in the central region of the tissue constructs.

Biochemical analysis of artificial skeletal muscle tissue constructs

For the functional evaluation of the C2C12/Bcl-2 muscle bundles, expression levels of the differentiation markers, myogenin, MHC, and tropomyosin were measured by western blot analysis (Fig. 5A). When equal amounts (30 μg) of total cell protein were applied for the assay, Bcl-2 overexpression was confirmed for C2C12/Bcl-2 (Dox+) muscle bundles, but no differences in the expression levels of myogenin, MHC, and tropomyosin were observed between C2C12/Bcl-2 (Dox−) and C2C12/Bcl-2 (Dox+) muscle bundles. In addition, no distinct differences were seen in creatin kinase activity between C2C12/Bcl-2 (Dox−) and C2C12/Bcl-2 (Dox+) muscle bundles (Fig. 5B). These results suggest that Bcl-2 overexpression specifically enhanced apoptotic tolerance and did not affect the biochemical properties of skeletal muscle tissue constructs.

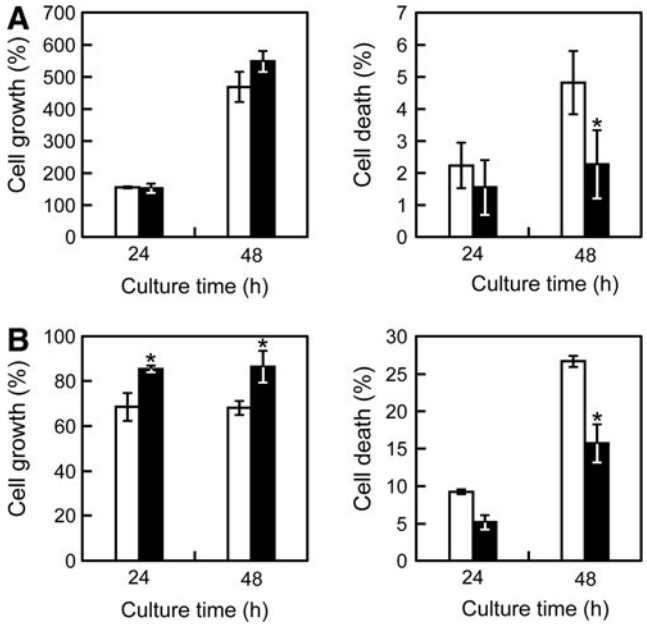

FIG. 2. The effect of Bcl-2 overexpression on cell growth and death under hypoxic or serum-depleted conditions. C2C12/Bcl-2 cells were cultured in hypoxic culture under 1% O_2 **(A)** or serum-depleted culture without fetal bovine serum **(B)**. The cells were collected periodically, and the numbers of viable and dead cells were counted using trypan blue dye-exclusion method to calculate the percentages of cell growth (left) and death (right). Open columns, without Dox addition; closed columns, with Dox addition. The data are expressed as mean ± SD ($n = 3$). *$p < 0.05$ versus the culture in the absence of Dox.

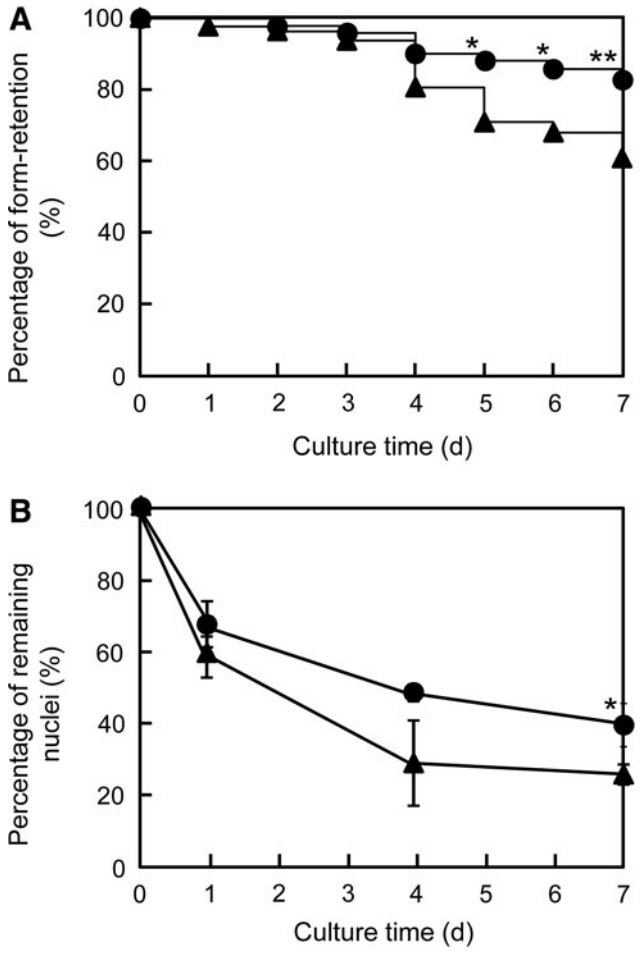

FIG. 3. Fabrication of artificial skeletal muscle tissue constructs. **(A)** Percentage of form retention for artificial skeletal muscle tissue constructs. The percentages of form retention for C2C12/Bcl-2 (Dox−) muscle bundles ($n = 82$) and C2C12/Bcl-2 (Dox+) muscle bundles ($n = 57$) were estimated according to the Kaplan–Meier method. **(B)** Percentage of remaining nuclei in artificial skeletal muscle tissue constructs during the differentiation culture. The data are expressed as mean ± SD of three constructs. Triangles, without Dox addition; circles, with Dox addition. *$p < 0.05$ and **$p < 0.01$ versus the culture in the absence of Dox.

Contractile properties of artificial skeletal muscle tissue constructs

To evaluate contractile properties, the artificial skeletal muscle tissue constructs were stimulated with electrical pulses. The force generation profiles in response to electrical stimulation are shown in Figure 6A. Twitch contractions occurred after low-frequency electrical stimulation, while tetanus was observed by repeated electrical stimulation with a higher frequency. These results indicate that the properties of C2C12/Bcl-2 bundles were qualitatively very similar to those of natural skeletal muscle tissues. The maximum contractile forces produced by the muscle bundles are shown in Figure 6B. The C2C12/Bcl-2 (Dox+) muscle bundles generated a significantly higher physical force by the twitch (18.3 ± 2.4 μN vs. 9.0 ± 3.0 μN; $p < 0.05$) and tetanus (34.5 ± 2.8 μN vs. 20.3 ± 4.8 μN; $p < 0.05$) contractions compared with the C2C12/Bcl-2 (Dox−) muscle bundles. However, there were no differences in specific force generation (1.02 and 0.97 kPa for Dox− and Dox+ muscle bundles, respectively) defined as contractile force of a tissue construct normalized by the cross-sectional area.

Discussion

We have developed a magnetic tissue fabrication technique in which MCL-labeled cells are accumulated to form 3D tissue-like structures through the application of a magnetic field.[11–15] The major advantage of this technology is that cell-dense tissues, which mimic normal tissue structures, can be induced to form within the construct, compared with conventional scaffold-based procedures. Particularly, high-cell density cultures with tight cell–cell contacts are necessary for skeletal muscle tissue formation to elicit a substantial function, as previously shown.[15] However, owing to the high cell density, there may be difficulties in the mass transport of nutrients and oxygen within the tissue constructs. This can cause necrosis/apoptosis within the tissue constructs, thereby limiting their size. Diffusion without blood vessels can support only a 100-μm thick viable cell layer,[30] whereas a human male quadriceps muscle is ~2–5-cm thick.[31] In the present study, C2C12/Bcl-2 (Dox−) muscle bundles had a viable cell layer that was ~100-μm thick from the surface to the necrotic central region, whereas the C2C12/Bcl-2 (Dox+) muscle bundles exhibited a fully viable area within the tissue construct that was ~200-μm thick. These results indicate that

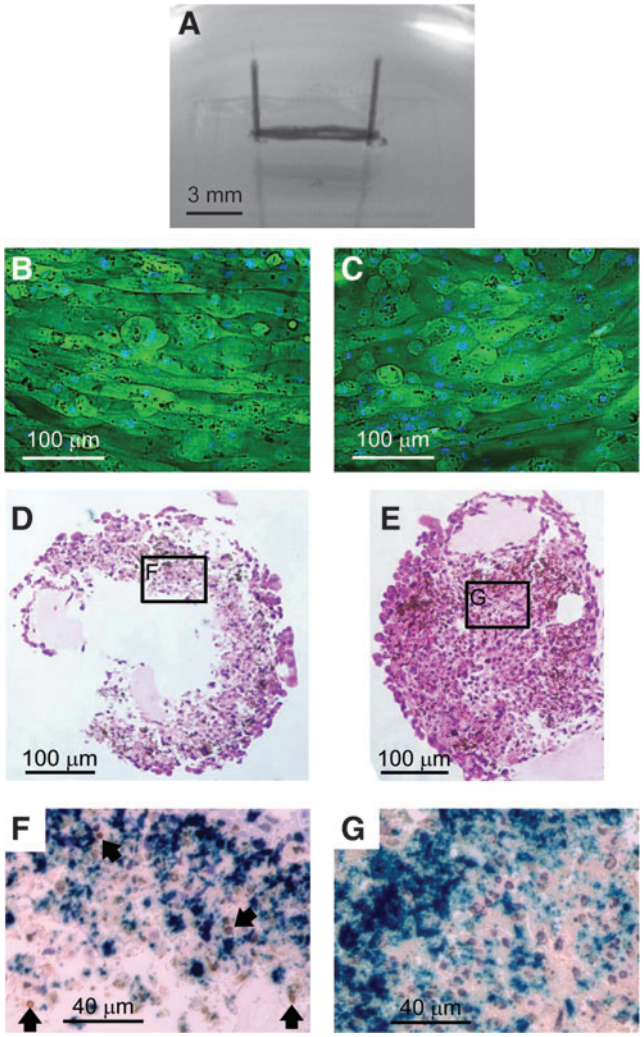

FIG. 4. Histological observation of artificial skeletal muscle tissue constructs on day 7. **(A)** Morphology of a representative artificial skeletal muscle tissue construct. The muscle bundle was anchored at each end with minuten pins. **(B, C)** Representative fluorescence images of the surface of C2C12/Bcl-2 (Dox−) **(B)** and C2C12/Bcl-2 (Dox+) **(C)** muscle bundles. Green, green fluorescent protein; blue, 4′,6-diamidino-2-phenylindole. **(D, E)** Typical hematoxylin and eosin staining images of cross-sections of C2C12/Bcl-2 (Dox−) **(D)** and C2C12/Bcl-2 (Dox+) **(E)** muscle bundles. The middle part of skeletal muscle tissue constructs between the pins was sliced to prepare the sections. **(F, G)** Bright-field micrographs of terminal deoxynucleotidyl transferase dUTP nick end labeling (TUNEL) staining of C2C12/Bcl-2 (Dox–) **(F)** and C2C12/Bcl-2 (Dox+) **(G)** muscle bundles. Locations of sections **(F)** and **(G)** in the muscle bundles are indicated in **(D)** and **(E)**, respectively. Blue, magnetite nanoparticles; brown, TUNEL-positive nuclei; purple, TUNEL-negative nuclei. Arrows indicate TUNEL-positive nuclei. Color images available online at www.liebertpub.com/tea

Bcl-2 gene transfer to myoblast cells has good potential for engineering high cell-dense and viable skeletal muscle tissue.

In the present study, 39% of C2C12/Bcl-2 (Dox−) muscle bundles ruptured during the differentiation culture. We previously reported that C2C12 cell sheets shrank in culture,[14] whereas NIH3T3 cell sheets did not. This suggests

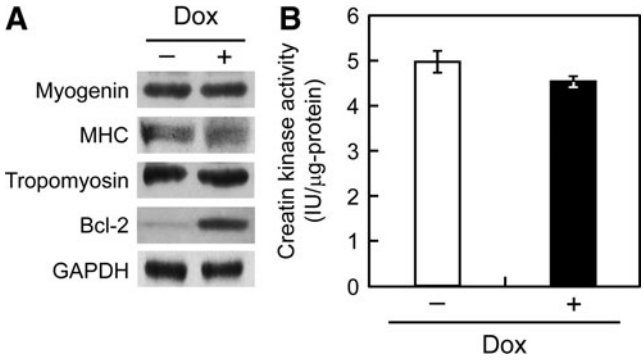

FIG. 5. Biochemical evaluation of artificial skeletal muscle tissue constructs. **(A)** Western blot analyses of muscle-specific proteins and Bcl-2 in artificial skeletal muscle tissue constructs. The expressions of myogenin, myosin heavy chain (MHC), tropomyosin, Bcl-2, and GAPDH in the muscle bundles were analyzed after 7 days of culture in the differentiation medium. **(B)** Creatine kinase activity of C2C12/Bcl-2 (Dox−) (open column) and C2C12/Bcl-2 (Dox+) (closed column) muscle bundles. The data are expressed as the mean ± SD of three bundles.

that the drastic shrinking of C2C12 cells is a feature of tissues composed of myoblast cells in which cell–cell interaction is crucial to differentiate into myotubes. The tension generated by muscle cells attached to collagen possibly causes shrinkage in collagen-embedded skeletal muscle constructs.[32] In the present study, muscle bundles were coated with the minimum volume of collagen/Matrigel solution, to prevent any effects that the collagen may have on shrinkage. The actual mechanism of tissue shrinkage has not yet been elucidated. Nevertheless, the yield of intact muscle bundles was

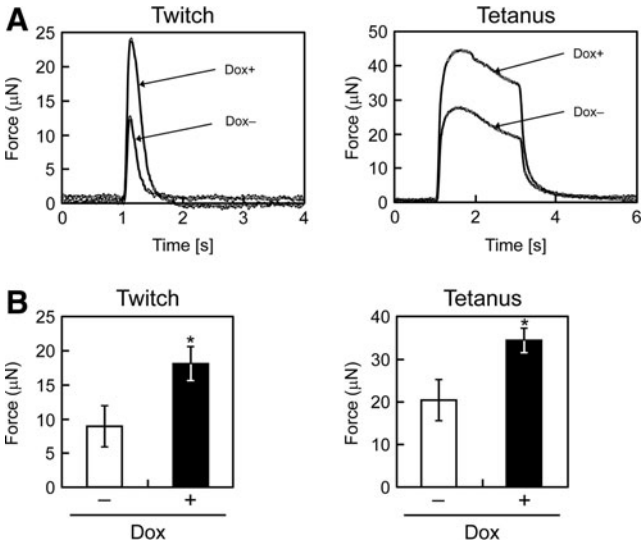

FIG. 6. Contractile properties of artificial skeletal muscle tissue constructs. **(A)** Representative peaks of the twitch force generated by the muscle bundles (left) and the fusion of tetanus of the muscle bundles (right) after 7 days of culture in the differentiation medium. **(B)** Maximum twitch (left) and tetanus (right) forces of the muscle bundles. The data are expressed as the means ± SD of three muscle bundles. *$p < 0.05$ versus C2C12/Bcl-2 (Dox−) muscle bundles.

effectively improved by Bcl-2 expression in the myoblast cells. Hinds *et al.*[3] reported that type I collagen-based muscle bundles exhibited a high degree of compaction and significant rupture, while fibrin-based muscle bundles remained intact even after 5 weeks of culture. Thus, the use of fibrin gels for Mag-TE may further improve the yield of C2C12 muscle bundles.

Interestingly, C2C12/Bcl-2 (Dox+) muscle bundles contracted to generate higher physical forces than did C2C12/Bcl-2 (Dox−) muscle bundles. To the best of our knowledge, this is the first report which demonstrates that *Bcl-2* gene transfer improves the contractile force generation of tissue-engineered skeletal muscle. In contrast, biochemical analysis revealed that there were no differences in expression levels of skeletal muscle differentiation markers between C2C12/Bcl-2 (Dox−) and C2C12/Bcl-2 (Dox+) muscle bundles. The 2D culture experiments under electrical stimulation disclosed that *Bcl-2* gene expression did not change the function of cell contractility. These results were also supported by the specific force generation; there were no differences in specific force generation between C2C12/Bcl-2 (Dox−) muscle bundles (1.02 kPa) and C2C12/Bcl-2 (Dox+) muscle bundles (0.97 kPa). From the H&E staining of cross-sections of C2C12/Bcl-2 (Dox+) muscle bundles, no apparent myotubes were observed at the central region of the bundles, even though the tissues were highly compact and highly cell dense. Di Carlo *et al.*[33] reported that hypoxia inhibited myogenic differentiation through accelerated MyoD degradation. These results indicate that the enhanced contractile force generation of the Bcl-2 overexpressing skeletal muscle bundles was attributable to the enhanced physical strength of highly packed cell-dense muscle bundles. In the present study, the twitch contractile force generated by C2C12/Bcl-2 (Dox+) muscle bundles was two-fold higher than that of C2C12/Bcl-2 (Dox−) muscle bundles. Strong contractile force generation of an artificial skeletal muscle tissue construct may be beneficial to the treatment of muscle disorders caused by traumatic injury and disease. In recent years, tissue-engineered skeletal muscle constructs have attracted much attention as bio-actuators.[34,35] When an artificial skeletal muscle can be applied as an actuator, it may exhibit excellent flexibility and highly efficient energy conversion.

Specific forces of C2C12/Bcl-2 muscle bundle constructs were two orders of magnitude less than that of normal adult muscle.[36,37] Hinds *et al.*[3] fabricated skeletal muscle tissue constructs composed of rat primary myoblasts by a hydrogel-based procedure using collagen/fibrin/Matrigel mixture. Although cell density of the tissue constructs (thickness, 2.7 mm; length, 20 mm; cell number, 6×10^6 cells) is not high compared with that of the C2C12/Bcl-2 muscle bundle constructs (thickness, 0.3–0.4 mm; length, 6 mm; cell number, 1×10^6 cells), the specific force generation of active muscle layer observed at the outer periphery of the tissue construct was high (9.4 kPa). This is probably due to the usage of rat primary myoblast cells and/or the longer period for differentiation (14 days). Skeletal muscle tissue constructs have also been fabricated using C2C12 cells by hydrogel-based procedures.[38,39] Khodabukus and Barr[38] prepared C2C12 constructs using fibrin gel. Their constructs generated a tetanic force of about 44 μN, which is at a similar level to the C2C12/Bcl-2 (Dox+) muscle bundles (44.1 μN). Rhim *et al.*[39] reported fabrication of C2C12 bioartifical muscles using collagen/Matrigel mixture. Cell density of the tissue constructs (thickness; 0.9–1.0 mm, length; 20 mm, cell number; 2×10^6 cells) is not high compared with that of the C2C12/Bcl-2 muscle bundle constructs. Specific force generation of the tissue constructs normalized by the cross-sectional area including hydrogel region was estimated as 1.0–1.3 kPa, showing the highest levels among artificial skeletal muscle constructs using C2C12 cells. Thus, the specific force generation of the C2C12/Bcl-2 muscle bundle constructs is comparable to the levels. From the microscopic observation of the tissue constructs, myotube formation was localized at the outer periphery of the tissue constructs. This indicates that the peripheral myotubes mainly contribute to contractile force generation of the skeletal muscle tissue constructs.

In conclusion, artificial skeletal muscle tissue constructs possessing highly packed viable cells were successfully fabricated using *Bcl-2* gene-engineered myoblast cells using Mag-TE. Bcl-2-overexpressing muscle bundles contracted in response to electrical stimuli and generated a significantly higher physical force than control muscle bundles. These findings represent the impact of anti-apoptotic gene transfer to myoblast cells on engineered skeletal muscle formation and function.

Acknowledgments

The authors thank Drs. Ohgushi and Takei for assisting the histological study. This work was supported in part by a Grant-in-Aid for Scientific Research (no. 23686121) from the Japan Society for the Promotion of Science and by a grant for the Global COE Program "Science for Future Molecular Systems" from the Ministry of Education, Culture, Sports, Science, and Technology, Japan.

Disclosure Statement

No competing financial interests exist.

References

1. Okano, T., and Matsuda, T. Tissue engineered skeletal muscle: preparation of highly dense, highly oriented hybrid muscular tissues. Cell Transplant **7,** 71, 1998.
2. Giraud, M.N., Ayuni, E., Cook, S., Siepe, M., Carrel, T.P., and Tevaearai, H.T. Hydrogel-based engineered skeletal muscle grafts normalize heart function early after myocardial infarction. Artif Organs **32,** 692, 2008.
3. Hinds, S., Bian, W., Dennis, R.G., and Bursac, N. The role of extracellular matrix composition in structure and function of bioengineered skeletal muscle. Biomaterials **32,** 3575, 2011.
4. Sato, M., Ito, A., Kawabe, Y., Nagamori, E., and Kamihira, M. Enhanced contractile force generation by artificial skeletal muscle tissues using IGF-I gene-engineered myoblast cells. J Biosci Bioeng **112,** 273, 2011.
5. Dennis, R.G., Kosnik, P.E., 2nd, Gilbert, M.E., and Faulkner, J.A. Excitability and contractility of skeletal muscle engineered from primary cultures and cell lines. Am J Physiol Cell Physiol **280,** C288, 2001.
6. Fujita, H., Shimizu, K., and Nagamori, E. Novel method for fabrication of skeletal muscle construct from the C2C12 myoblast cell line using serum-free medium AIM-V. Biotechnol Bioeng **103,** 1034, 2009.
7. Saxena, A.K., Marler, J., Benvenuto, M., Willital, G.H., and Vacanti, J.P. Skeletal muscle tissue engineering using

isolated myoblasts on synthetic biodegradable polymers: preliminary studies. Tissue Eng **5,** 525, 1999.
8. Gawlitta, D., Boonen, K.J., Oomens, C.W., Baaijens, F.P., and Bouten, C.V. The influence of serum-free culture conditions on skeletal muscle differentiation in a tissue-engineered model. Tissue Eng Part A **14,** 161, 2008.
9. Moon du, G., Christ, G., Stitzel, J.D., Atala, A., and Yoo, J.J. Cyclic mechanical preconditioning improves engineered muscle contraction. Tissue Eng Part A **14,** 473, 2008.
10. Singh, D., Nayak, V., and Kumar, A. Proliferation of myoblast skeletal cells on three-dimensional supermacroporous cryogels. Int J Biol Sci **6,** 371, 2010.
11. Ito, A., Hayashida, M., Honda, H., Hata, K., Kagami, H., Ueda, M., and Kobayashi, T. Construction and harvest of multilayered keratinocyte sheets using magnetite nanoparticles and magnetic force. Tissue Eng **10,** 873, 2004.
12. Ito, A., Shinkai, M., Honda, H., and Kobayashi, T. Medical application of functionalized magnetic nanoparticles. J Biosci Bioeng **100,** 1, 2005.
13. Akiyama, H., Ito, A., Kawabe, Y., and Kamihira, M. Genetically engineered angiogenic cell sheets using magnetic force-based gene delivery and tissue fabrication techniques. Biomaterials **31,** 1251, 2010.
14. Yamamoto, Y., Ito, A., Kato, M., Kawabe, Y., Shimizu, K., Fujita, H., Nagamori, E., and Kamihira, M. Preparation of artificial skeletal muscle tissues by a magnetic force-based tissue engineering technique. J Biosci Bioeng **108,** 538, 2009.
15. Yamamoto, Y., Ito, A., Fujita, H., Nagamori, E., Kawabe, Y., and Kamihira, M. Functional evaluation of artificial skeletal muscle tissue constructs fabricated by a magnetic force-based tissue engineering technique. Tissue Eng Part A **17,** 107, 2011.
16. Levenberg, S., Rouwkema, J., Macdonald, M., Garfein, E.S., Kohane, D.S., Darland, D.C., Marini, R., van Blitterswijk, C.A., Mulligan, R.C., D'Amore, P.A., and Langer, R. Engineering vascularized skeletal muscle tissue. Nat Biotechnol **23,** 879, 2005.
17. Lu, Y., Shansky, J., Del Tatto, M., Ferland, P., Wang, X., and Vandenburgh, H. Recombinant vascular endothelial growth factor secreted from tissue-engineered bioartificial muscles promotes localized angiogenesis. Circulation **104,** 594, 2001.
18. De Coppi, P., Delo, D., Farrugia, L., Udompanyanan, K., Yoo, J.J., Nomi, M., Atala, A., and Soker, S. Angiogenic gene-modified muscle cells for enhancement of tissue formation. Tissue Eng **11,** 1034, 2005.
19. Leach, R.M., and Treacher, D.F. Oxygen transport-2. Tissue hypoxia. BMJ **317,** 1370, 1998.
20. Brunelle, J.K., and Chandel, N.S. Oxygen deprivation induced cell death: an update. Apoptosis **7,** 475, 2002.
21. Hengartner, M.O. The biochemistry of apoptosis. Nature **407,** 770, 2000.
22. Chinnaiyan, A.M., Orth, K., O'Rourke, K., Duan, H., Poirier, G.G., and Dixit, V.M. Molecular ordering of the cell death pathway. Bcl-2 and Bcl-xL function upstream of the CED-3-like apoptotic proteases. J Biol Chem **271,** 4573, 1996.
23. Yung, C.W., Barbari, T.A., and Bentley, W.E. Counteracting apoptosis and necrosis with hypoxia responsive expression of Bcl-2Delta. Metab Eng **8,** 483, 2006.
24. Ito, A., Kiyohara, T., Kawabe, Y., Ijima, H., and Kamihira, M. Enhancement of cell function through heterotypic cell-cell interactions using E-cadherin-expressing NIH3T3 cells. J Biosci Bioeng **105,** 679, 2008.
25. Penno, C.A., Kawabe, Y., Ito, A., and Kamihira, M. Production of recombinant human erythropoietin/Fc fusion protein by genetically manipulated chickens. Transgenic Res **19,** 187, 2010.
26. Hotta, A., Saito, Y., Kyogoku, K., Kawabe, Y., Nishijima, K., Kamihira, M., and Iijima, S. Characterization of transient expression system for retroviral vector production. J Biosci Bioeng **101,** 361, 2006.
27. Shinkai, M., Yanase, M., Honda, H., Wakabayashi, T., Yoshida, J., and Kobayashi, T. Intracellular hyperthermia for cancer using magnetite cationic liposomes: *in vitro* study. Jpn J Cancer Res **87,** 1179, 1996.
28. Kaplan, E.L., and Meier, P. Nonparametric estimation from incomplete observations. J Am Stat Assoc **53,** 457, 1958.
29. Ito, A., Takizawa, Y., Honda, H., Hata, K., Kagami, H., Ueda, M., and Kobayashi, T. Tissue engineering using magnetite nanoparticles and magnetic force: heterotypic layers of cocultured hepatocytes and endothelial cells. Tissue Eng **10,** 833, 2004.
30. Tsai, A.G., Friesenecker, B., Mazzoni, M.C., Kerger, H., Buerk, D.G., Johnson, P.C., and Intaglietta, M. Microvascular and tissue oxygen gradients in the rat mesentery. Proc Natl Acad Sci U S A **95,** 6590, 1998.
31. Pillen, S., Arts, I.M., and Zwarts, M.J. Muscle ultrasound in neuromuscular disorders. Muscle Nerve **37,** 679, 2008.
32. Yan, W., George, S., Fotadar, U., Tyhovych, N., Kamer, A., Yost, M.J., Price, R.L., Haggart, C.R., Holmes, J.W., and Terracio, L. Tissue engineering of skeletal muscle. Tissue Eng **13,** 2781, 2007.
33. Di Carlo, A., De Mori, R., Martelli, F., Pompilio, G., Capogrossi, M.C., and Germani, A. Hypoxia inhibits myogenic differentiation through accelerated MyoD degradation. J Biol Chem **279,** 16332, 2004.
34. Feinberg, A.W., Feigel, A., Shevkoplyas, S.S., Sheehy, S., Whitesides, G.M., and Parker, K.K. Muscular thin films for building actuators and powering devices. Science **317,** 1366, 2007.
35. Fujita, H., Van Dau, T., Shimizu, K., Hatsuda, R., Sugiyama, S., and Nagamori, E. Designing of a Si-MEMS device with an integrated skeletal muscle cell-based bio-actuator. Biomed Microdevices **13,** 123, 2011.
36. Close, R.I. Dynamic properties of mammalian skeletal muscles. Physiol Rev **52,** 129, 1972.
37. Isaacson, A., Hinkes, M.J., and Taylor, S.R. Contracture and twitch potentiation of fast and slow muscles of the rat at 20 and 37° C. Am J Physiol **218,** 33, 1970.
38. Khodabukus, A., and Baar, K. Regulating fibrinolysis to engineer skeletal muscle from the C2C12 cell line. Tissue Eng Part C Methods **15,** 501, 2009.
39. Rhim, C., Cheng, C.S., Kraus, W.E., and Truskey, G.A. Effect of microRNA modulation on bioartificial muscle function. Tissue Eng Part A **16,** 3589, 2010.

Address correspondence to:
Masamichi Kamihira, Ph.D.
Department of Chemical Engineering
Faculty of Engineering
Kyushu University
744 Motooka, Nishi-ku
Fukuoka 819-0395
Japan

E-mail: kamihira@chem-eng.kyushu-u.ac.jp

Received: December 22, 2011
Accepted: August 13, 2012
Online Publication Date: November 21, 2012